

Seismic reflection and transmission coefficients of a single layer sandwiched between two dissimilar poroelastic solids

Manjeet Kumari¹ · Mahabir Singh Barak¹ · Manjeet Kumar²

Received: 24 February 2017 / Published online: 8 November 2017
© The Author(s) 2017. This article is an open access publication

Abstract The seismic reflection and transmission characteristics of a single layer sandwiched between two dissimilar poroelastic solids saturated with two immiscible viscous fluids are investigated. The sandwiched layer is modeled as a porous solid with finite thickness. The propagation of waves is represented with potential functions. The displacements of particles in different phases of the aggregate are defined in terms of these potential functions. Due to the presence of viscosity in pore fluids, the reflected and transmitted waves are inhomogeneous in nature, i.e., with different directions of propagation and attenuation. The closed-form analytical expressions for reflection and transmission coefficients are derived theoretically for appropriate boundary conditions. These expressions are calculated as a non-singular system of linear algebraic equations and depend on the various parameters involved in this non-singular system. Hence, numerical examples are studied to determine the effects of various properties of the sandwich layer on reflection and transmission coefficients. The essential features of layer thickness, incident direction, wave frequency, liquid

saturation and capillary pressure of the porous layer on reflection and transmission coefficients are depicted graphically and discussed. The analysis shows that reflection and transmission coefficients are strongly associated with incident direction and various properties of the porous layer.

Keywords Sandwiched layer · Immiscible pore fluids · Inhomogeneous wave · Reflection and transmission coefficients

1 Introduction

In general, earth is a layered structure with different elastic properties. Thus, propagation of seismic waves through such a layered structure is influenced very much by these elastic properties. The nature of these layers present in the interior of earth's crust has not yet been addressed completely. Therefore, it is necessary to consider the various studies to determine the actual internal structure of earth and the various phases such as oil, gases and hydrocarbons embedded in the earth. The problem of reflection and transmission of seismic waves at a sandwiched layer is an important phenomenon due to its practical applications in earthquake engineering, geophysics, seismology, petroleum engineering and hydrology. During the past several decades, most of the studies on reflection and transmission phenomena have preferred to use a single interface, for example Pride et al. (1992), Kaynia and Banerjee (1993), Gurevich and Schoenberg (1999), Denneman et al. (2002), Sharma (2008, 2013), Tomar and Arora (2006), Arora and Tomar (2007), Yeh et al. (2010), Sharma and Kumar (2011), Chen et al. (2012), Kumar and Saini (2012, 2016),

✉ Manjeet Kumar
manjit.msc@gmail.com

Manjeet Kumari
manjeet.aryan17@gmail.com

Mahabir Singh Barak
ms_barak@igu.ac.in

¹ Department of Mathematics, Indira Gandhi University, Meerpur, Rewari-122505, India

² Department of Mathematics, C.M.R.J Govt. College, Ellenabad, Sirsa-125102, India

Kumar and Sharma (2013), Kumar and Kumari (2014). The latest book by Carcione (2014) is also recommended for relevant references and detailed procedures. However, to the best of our knowledge, in view the importance of the transition layer, only a few limited efforts have been made to study the phenomenon of reflection and transmission of plane waves at a layer sandwiched between two dissimilar media. Some of the recent studies on reflection and transmission of seismic waves through a transition layer have been carried out by various authors including Sinha (1964), Cerveny and Vanek (1974), Kuo (1992), Ainslie (1996), Wang et al. (2013), Lyu et al. (2014), Sahu et al. (2015) and Paswan et al. (2016). Recently, Corredor et al. (2014) studied the effects of layer thickness on reflection and transmission coefficients of a single layer sandwiched between two dissimilar poroelastic media. They also discussed several special cases. Chen et al. (2015) studied the reflection of acoustic waves from the elastic seabed with an overlying gassy poroelastic layer. They studied the influences of poroelastic layer thickness, wave frequency, incident direction and liquid saturation on reflection characteristics.

To the best of our knowledge, until now the problem of reflection and transmission of plane waves at the surface of a layer sandwiched between two dissimilar porous solids saturated with two immiscible viscous fluids has not been investigated. Generally, it is observed that natural rocks are composed of multi-fluid porous solids. The phenomenon of wave propagation is generally affected by the nature of such rocks. In the present work, the complete reflection–transmission phenomenon across a poroelastic layer sandwiched between two dissimilar porous solids saturated with two immiscible viscous fluids is investigated. This type of study is motivated by the problems faced by the oil industry, where the desired product is usually found in the form of multiple fluids. The mathematical model presented in this article is based on the continuum mixture theory of Tuncay and Corapcioglu (1997). Corredor et al. (2014) studied the reflection and transmission coefficients of a single layer embedded between two dissimilar porous solid saturated with a single fluid. It is based on the poroelastic theory of Biot. The present work generalizes reflection/transmission phenomenon studied by Corredor et al. (2014) to the reflection/transmission phenomena across a poroelastic layer sandwiched between two dissimilar porous solids saturated with two immiscible viscous fluids.

In this study, the propagation of waves is represented with potential functions. The displacement of particles in different phases of the aggregate is defined in terms of these potential functions. All the poroelastic media are dissipative due to the presence of viscosity in pore fluids. Hence, the propagation of plane waves in such media is represented by inhomogeneous waves, i.e., different

directions of propagation and attenuation. Thus, the incident wave is an inhomogeneous wave specified by two angles, one for the propagation direction and the other for its deviation from the attenuation direction. The closed-form expressions for reflection and transmission coefficients are derived theoretically for appropriate boundary conditions. These expressions are calculated as a non-singular system of linear algebraic equations and depend on various parameters involved in this non-singular system. Hence, numerical examples are studied to determine the effects of various properties of the sandwich layer on reflection and transmission coefficients. The influences of layer thickness, liquid saturation and capillary pressure of the porous layer, incident direction and wave frequency on reflection and transmission coefficients are depicted graphically and discussed.

2 Basics equations

Following Tuncay and Corapcioglu (1997), the equations of motion for two-phase immiscible viscous fluid flows in deformable porous media, in the absence of body forces, are defined as follows

$$\delta_0 \tau_{ij,j} = \delta_0 \rho_0 \ddot{u}_i + d_1(\dot{u}_i - \dot{v}_i) + d_2(\dot{u}_i - \dot{w}_i), \tag{1}$$

$$-\delta_1 p_{,i}^{(1)} = \delta_1 \rho_1 \ddot{v}_i + d_1(\dot{v}_i - \dot{u}_i), \tag{2}$$

$$-\delta_2 p_{,i}^{(2)} = \delta_2 \rho_2 \ddot{w}_i + d_2(\dot{w}_i - \dot{u}_i), \tag{3}$$

where u_i, v_i and w_i denote the components of displacements of solid, first fluid and second fluid particles, respectively. $p^{(1)}, p^{(2)}$ are pressures in fluid phases, and τ_{ij} is the stress tensor for the drained porous frame. ρ 's are intrinsic densities of constituents. Dots over these vectors denote partial time derivatives. A comma before an index implies partial differentiation in space. δ_0, δ_1 and δ_2 are the volume fractions of the solid, first and second fluid phases, respectively. $\delta_0 = 1 - f, \delta_1 = (1 - \sigma)f, \delta_2 = f\sigma$ with $\delta_0 + \delta_1 + \delta_2 = 1$, where σ is the fraction of second fluid saturation in connected pore space and f is porosity. $d_1 (= \eta_1 \delta_1^2 / \chi_0 k_{r1})$ and $d_2 (= \eta_2 \delta_2^2 / \chi_0 k_{r2})$ are the dissipation coefficients of first and second fluid phases, respectively. These coefficients involve relative permeabilities (k_{r1}, k_{r2}) and viscosities (ν_1, ν_2) of the corresponding phases and the intrinsic permeability of the composite medium χ_0 . The relative permeabilities (k_{r1}, k_{r2}) for current model are given as follows (Lo et al. 2005): $k_{r1} = (1 - \sigma)^\chi [1 - \sigma^{\frac{n}{n-1}}]^{\frac{2(n-1)}{n}}$, $k_{r2} = \sigma^\chi [1 - \{1 - \sigma^{\frac{n}{n-1}}\}^{\frac{n-1}{n}}]^2$, where n and χ are fitting parameters. Following Tuncay and Corapcioglu (1997), the constitutive relations for stresses in the porous matrix and fluid pressures in the pore space are given by

$$\delta_0 \tau_{ij} = \left(a_{11} \nabla \cdot \vec{u} + a_{12} \nabla \cdot \vec{v} + a_{13} \nabla \cdot \vec{w} \right) \delta_{ij} + G \left(u_{i,j} + u_{j,i} - \frac{2}{3} u_{k,k} \delta_{ij} \right), \quad (4)$$

$$- \delta_1 p^{(1)} = (a_{21} \nabla \cdot \vec{u} + a_{22} \nabla \cdot \vec{v} + a_{23} \nabla \cdot \vec{w}) \delta_{ij}, \quad (5)$$

$$- \delta_2 p^{(2)} = (a_{31} \nabla \cdot \vec{u} + a_{32} \nabla \cdot \vec{v} + a_{33} \nabla \cdot \vec{w}) \delta_{ij}, \quad (6)$$

where δ_{ij} is the Kronecker symbol. The coefficients a_{ij} ($= a_{ji}$) denote the elastic constants and are given by

$$a_{11} = K_0, \quad a_{12} = K_1 \delta_0 (1 - \sigma) (K_c + K_2) / K,$$

$$a_{13} = K_2 \delta_0 \sigma (K_c + K_1) / K,$$

$$a_{22} = K_1 \delta_1 ((1 - \sigma) K_2 + K_c) / K, \quad a_{23} = K_1 K_2 (1 - \sigma) \delta_2 / K,$$

$$a_{33} = K_2 \delta_2 (K_1 \sigma + K_c) / K, \quad K = K_1 \sigma + K_c + K_2 (1 - \sigma),$$

where K_1 and K_2 are the bulk moduli of first and second fluid phases, respectively, whereas K_0 is bulk modulus of the porous frame or drained matrix. G is the shear modulus of the porous solid. $K_c = \sigma K_{\text{cap}}$, where K_{cap} is the equivalent bulk modulus (Garg and Nayfeh 1986) for macroscopic capillary pressure between wetting and non-wetting fluids.

Following Kumar and Saini (2012), the displacement potentials φ_i , ($i = 1, 2, 3, 4$), represent the propagation of P_1, P_2, P_3, SV waves with velocities V_1, V_2, V_3, V_4 , respectively. The velocities (V_1, V_2, V_3) of longitudinal waves are derived from the three roots of a cubic equation in V^2 , given by

$$DV^6 + CV^4 + BV^2 + A = 0. \quad (7)$$

The various coefficients in this cubic equation are given by

$$A = a_{11}^* A_3 + a_{12} A_1 + a_{13} A_2,$$

$$B = a_{11}^* B_3 + A_5 A_3 + a_{12} B_1 + a_{13} B_2 - \chi_1 A_1 - \chi_2 A_2,$$

$$C = a_{11}^* C_3 + A_5 B_3 + a_{12} C_1 + a_{13} C_2 - \chi_1 B_1 - \chi_2 B_2,$$

$$D = A_5 C_3 - \chi_1 C_1 - \chi_2 C_2,$$

where

$$A_1 = a_{23} a_{13} - a_{12} a_{33}, \quad A_2 = a_{12} a_{23} - a_{13} a_{22},$$

$$A_3 = a_{22} a_{33} - a_{23} a_{23},$$

$$B_1 = a_{33} \chi_1 - a_{12} A_2 - a_{23} \chi_2, \quad B_2 = a_{22} \chi_2 - a_{13} A_1 - a_{23} \chi_1,$$

$$B_3 = a_{22} A_2 + a_{33} A_1,$$

$$C_1 = A_2 \chi_1, \quad C_2 = A_1 \chi_2, \quad C_3 = A_1 A_2, \quad a_{11}^* = a_{11} + \frac{4}{3} G,$$

and

$$\chi_1 = \frac{l}{\omega} d_1, \quad \chi_2 = \frac{l}{\omega} d_2, \quad A_1 = \delta_1 \rho_1 + \chi_1,$$

$$A_2 = \delta_2 \rho_2 + \chi_2,$$

where $l = \sqrt{-1}$ and ω is angular frequency. The coupling coefficients between the potentials of longitudinal waves are given by

$$\mu_j = \frac{A_1 - B_1 V_j^2 + C_1 V_j^4}{A_3 - B_3 V_j^2 + C_3 V_j^4}, \quad \lambda_j = \frac{A_2 - B_2 V_j^2 + C_2 V_j^4}{A_3 - B_3 V_j^2 + C_3 V_j^4},$$

$$(j = 1, 2, 3).$$

The shear wave velocity V_4 and coupling coefficients (Γ_1, Γ_2) are given by

$$V_4^2 = \frac{G}{A_0 - \chi_1 \Gamma_1 - \chi_2 \Gamma_2}, \quad \Gamma_1 = \frac{\chi_1}{A_1}, \quad \Gamma_2 = \frac{\chi_2}{A_2},$$

$$A_0 = \delta_0 \rho_0 + \chi_1 + \chi_2.$$

3 Displacements

For two-dimensional motion in the $x-z$ plane, the displacement components of solid and fluid phases are given by

$$u_x = \sum_{j=1}^3 \frac{\partial \varphi_j}{\partial x} - \frac{\partial \varphi_4}{\partial z}, \quad u_z = \sum_{j=1}^3 \frac{\partial \varphi_j}{\partial z} + \frac{\partial \varphi_4}{\partial x}, \quad (8)$$

$$v_x = \sum_{j=1}^3 \mu_j \frac{\partial \varphi_j}{\partial x} - \Gamma_1 \frac{\partial \varphi_4}{\partial z}, \quad v_z = \sum_{j=1}^3 \mu_j \frac{\partial \varphi_j}{\partial z} + \Gamma_1 \frac{\partial \varphi_4}{\partial x}, \quad (9)$$

$$w_x = \sum_{j=1}^3 \lambda_j \frac{\partial \varphi_j}{\partial x} - \Gamma_2 \frac{\partial \varphi_4}{\partial z}, \quad w_z = \sum_{j=1}^3 \lambda_j \frac{\partial \varphi_j}{\partial z} + \Gamma_2 \frac{\partial \varphi_4}{\partial x}. \quad (10)$$

4 Formulation of the problem

We consider a poroelastic layer sandwiched between two dissimilar poroelastic solids saturated with two immiscible viscous fluids. This poroelastic layer is considered as solid matrix (or skeleton) whose pores are filled with two immiscible viscous fluids. Hence, this system consists of three dissimilar poroelastic media designated by Ω_j , ($j = 1, 2, 3$) as shown in Fig. 1. A rectangular Cartesian coordinate system (x, y, z) is chosen with the z -axis directed vertically downwards and the x -axis considered as the horizontal direction. Let $z = 0$ and $z = h$ represent two plane interfaces separating the media Ω_1, Ω_2 and Ω_3 , respectively. Hence, the poroelastic solid Ω_1 occupies the region $-\infty < z < 0$, poroelastic layer Ω_2 occupies the region $0 < z < h$, and poroelastic solid Ω_3 occupies the region $h < z < \infty$.

5 Boundary conditions

Boundary conditions are considered to determine the unknown complex amplitudes of various reflected and transmitted waves. These boundary conditions concerning the displacements of solid and fluid particles, normal and

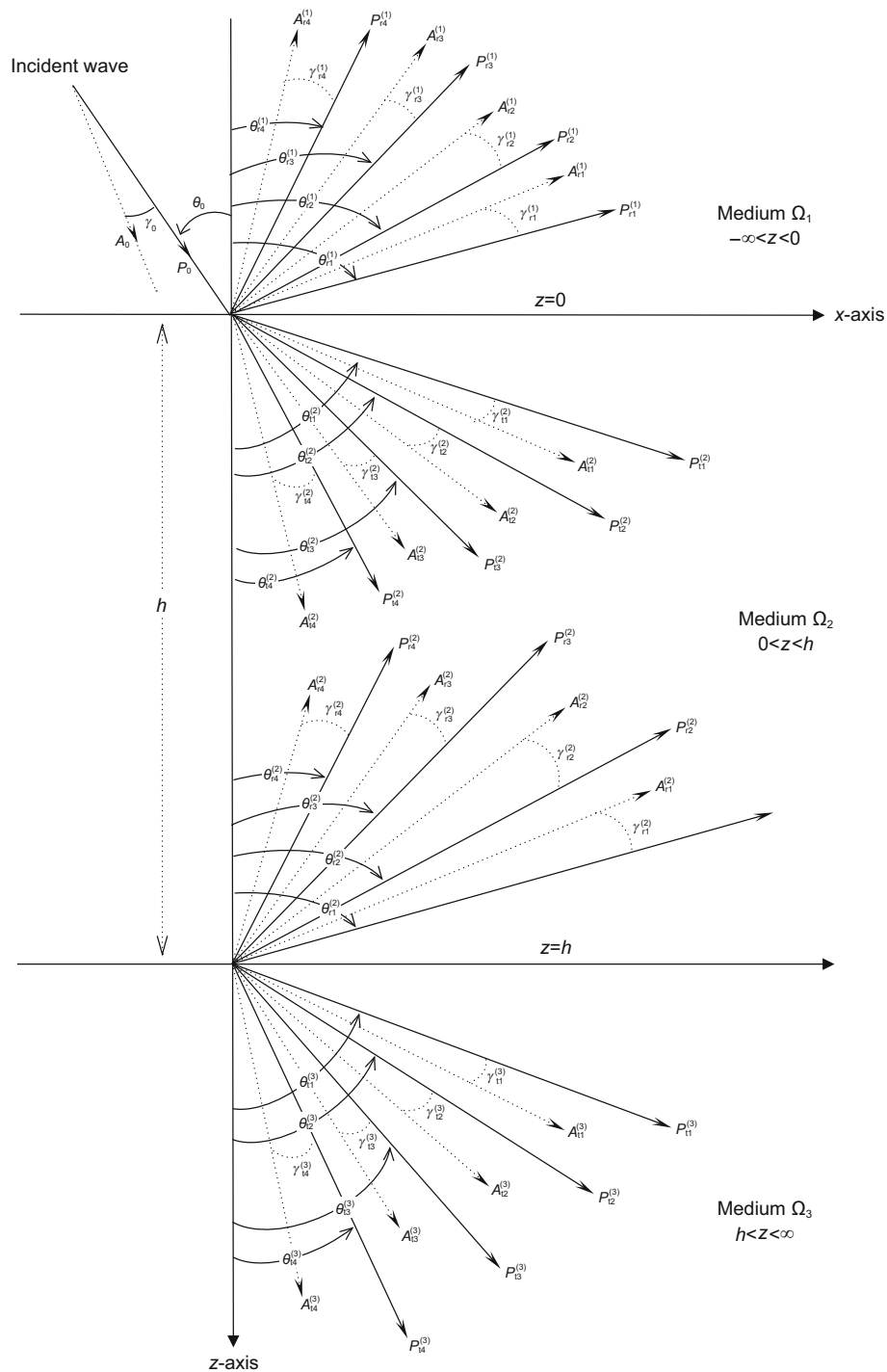


Fig. 1 Geometry of the problem

shear stresses, and fluids pressure need to ensure continuity at the interfaces located at $z = 0$ and $z = h$. Therefore, the boundary conditions at the interfaces (Dutta and Ode 1983; Santos et al. 2004; Corredor et al. 2014), in the present formulations, are given by

$$\begin{aligned}
 (\delta_0 \tau_{zz})^{(m)} &= (\delta_0 \tau_{zz})^{(m+1)}, & (\delta_0 \tau_{zx})^{(m)} &= (\delta_0 \tau_{zx})^{(m+1)}, \\
 (-\delta_1 p^{(1)})^{(m)} &= (-\delta_1 p^{(1)})^{(m+1)}, \\
 (-\delta_2 p^{(2)})^{(m)} &= (-\delta_2 p^{(2)})^{(m+1)}, \\
 u_x^{(m)} &= u_x^{(m+1)}, & u_z^{(m)} &= u_z^{(m+1)}, & v_z^{(m)} &= v_z^{(m+1)}, \\
 w_z^{(m)} &= w_z^{(m+1)}, & m &= 1, 2.
 \end{aligned}
 \tag{11}$$

The super-index (m) denotes the any variable associated with the medium Ω_m .

6 Reflection and transmission coefficients

In the present study, our goal is to analyze the reflection and transmission coefficients of a poroelastic layer sandwiched between two dissimilar poroelastic solids saturated with two immiscible fluids. A plane wave, either P_1 or SV , is incident on the plane interface $z = 0$ with an angular frequency ω and an angle of incidence θ_0 with respect to vertical z -axis. This incidence results in four reflected waves generated in the poroelastic medium Ω_1 . Furthermore, four waves from the upper interface (i.e., $z = 0$) and four reflected waves from the lower interface (i.e., $z = h$) are generated in the poroelastic layer Ω_2 and four transmitted waves exist in the poroelastic medium Ω_3 , as shown in Fig. 1. Hence, as a result of multiple reflections at the boundaries of the layer, eight resulting waves with different directions of propagation and attenuation are developed. The procedure used in the present work to determine the reflection and transmission coefficients of plane waves is illustrated by Brekhovskikh (1960), p. 45. This recursive approach is used by various authors including Carcione (2001), Wang et al. (2013), Lyu et al. (2014), Corredor et al. (2014), Chen et al. (2015, 2017), Sahu et al. (2015), Bai et al. (2015, 2016), Paswan et al. (2016), Feng et al. (2016). All the poroelastic media are dissipative due to the presence of viscosity in pore fluids. Hence, the propagation of plane waves in such a medium is represented by inhomogeneous waves, i.e., with different directions of propagation and attenuation. Thus, the incidence of an inhomogeneous wave at the boundary $z = 0$ is specified through its propagation direction θ_0 and attenuation angle γ_0 . In the x - z plane, θ_0 is the angle that propagation vector \vec{P}_0 of the incident wave makes with the z -axis and γ_0 is the angle between propagation vector (\vec{P}_0) and attenuation vector (\vec{A}_0).

In terms of these angles, the complex wave number k is written as (Borcherdt 1982),

$$k = |\vec{P}_0| \sin \theta_0 - i |\vec{A}_0| \sin(\theta_0 - \gamma_0), \tag{12}$$

where for incident wave of velocity V_0 , we have

$$|\vec{P}_0|^2 = \frac{1}{2} \left[\Re \left(\frac{\omega^2}{V_0^2} \right) + \sqrt{\left\{ \left(\Re \left(\frac{\omega^2}{V_0^2} \right) \right)^2 + \left(\Im \left(\frac{\omega^2}{V_0^2} \right) \right)^2 \right\} / \cos^2 \gamma_0} \right], \tag{13}$$

$$|\vec{A}_0|^2 = \frac{1}{2} \left[-\Re \left(\frac{\omega^2}{V_0^2} \right) + \sqrt{\left\{ \left(\Re \left(\frac{\omega^2}{V_0^2} \right) \right)^2 + \left(\Im \left(\frac{\omega^2}{V_0^2} \right) \right)^2 \right\} / \cos^2 \gamma_0} \right]. \tag{14}$$

Then, the displacement potential for the incident wave is defined as

$$\phi_0 = F_0 \exp(\vec{A}_0 \cdot \vec{r}) \exp(i\vec{P}_0 \cdot \vec{r} - \omega t), \tag{15}$$

The propagation vector \vec{P}_0 and attenuation vector \vec{A}_0 are defined as

$$\vec{P}_0 = k_R \hat{x} + d_{0R} \hat{z}, \quad \vec{A}_0 = -k_I \hat{x} - d_{0I} \hat{z},$$

$$d_0 = \pm p.v. \left[\left(\frac{\omega}{V_0} \right)^2 - \left(k^{(1)} \right)^2 \right]^{1/2}, \quad \vec{r} = x \hat{x} + z \hat{z},$$

where \hat{x} and \hat{z} denote unit (or coordinate) vectors along x -axis and z -axis, respectively. F_0 is the amplitude of the incident wave. Subscripts R and I denote the real and imaginary parts of the corresponding complex quantities.

Following Borcherdt (1982), the displacement potential functions of reflected and transmitted waves can be expressed as

(1) In the poroelastic solid Ω_1 ($-\infty < z < 0$)

$$\phi_j^{(1)} = F_{rj}^{(1)} \exp(\vec{A}_{rj}^{(1)} \cdot \vec{r}) \exp\{i(\vec{P}_{rj}^{(1)} \cdot \vec{r} - \omega t)\}, \tag{16}$$

$(j = 1, 2, 3, 4),$

where arbitrary constants $F_{rj}^{(1)}$, ($j = 1, 2, 3, 4$), represent the amplitudes of reflected P_1, P_2, P_3, SV waves, respectively.

The propagation vectors $\vec{P}_{rj}^{(1)}$ and attenuation vectors $\vec{A}_{rj}^{(1)}$ are defined as

$$\vec{P}_{rj}^{(1)} = k_R^{(1)} \hat{x} - d_{rjR}^{(1)} \hat{z}, \quad \vec{A}_{rj}^{(1)} = -k_I^{(1)} \hat{x} + d_{rjI}^{(1)} \hat{z},$$

$$d_{rj}^{(1)} = \pm p.v. \left[\left(\frac{\omega}{V_j^{(1)}} \right)^2 - \left(k^{(1)} \right)^2 \right]^{1/2},$$

where $p.v.$ denotes the principal value of the complex quantity derived from the square root. The sign of $d_{rj}^{(1)}$ is chosen to ensure the decay of associated reflected wave along negative z -direction, i.e., a positive value for imaginary part of $d_{rj}^{(1)}$. Wave number $k^{(1)} (= k_R^{(1)} + ik_I^{(1)})$ is a complex quantity such that $k_R^{(1)} \geq 0$ defines the propagation in positive x -direction.

(2) In the poroelastic layer Ω_2 ($0 < z < h$)

$$\phi_j^{(2)} = F_{tj}^{(2)} \exp(\vec{A}_{tj}^{(2)} \cdot \vec{r}) \exp\{i(\vec{P}_{tj}^{(2)} \cdot \vec{r} - \omega t)\} + F_{rj}^{(2)} \exp(\vec{A}_{rj}^{(2)} \cdot \vec{r}) \exp\{i(\vec{P}_{rj}^{(2)} \cdot \vec{r} - \omega t)\}, \tag{17}$$

$(j = 1, 2, 3, 4),$

where arbitrary constants $F_{rj}^{(2)}$ ($F_{tj}^{(2)}$), ($j = 1, 2, 3, 4$), represent the amplitudes of reflected (transmitted) P_1, P_2, P_3, SV waves, respectively.

The propagation vectors $(\vec{P}_{rj}^{(2)}, \vec{P}_{ij}^{(2)})$ and attenuation vectors $(\vec{A}_{rj}^{(2)}, \vec{A}_{ij}^{(2)})$ are defined as

$$\begin{aligned} \vec{P}_{rj}^{(2)} &= k_R^{(2)} \hat{x} - d_{rjR}^{(2)} \hat{z}, & \vec{P}_{ij}^{(2)} &= k_R^{(2)} \hat{x} + d_{ijR}^{(2)} \hat{z}, \\ \vec{A}_{rj}^{(2)} &= -k_I^{(2)} \hat{x} + d_{rjI}^{(2)} \hat{z}, & \vec{A}_{ij}^{(2)} &= -k_I^{(2)} \hat{x} - d_{ijI}^{(2)} \hat{z}, \\ d_{rj}^{(2)} &= \pm p.v. \left[\left(\frac{\omega}{V_j^{(2)}} \right)^2 - \left(k^{(2)} \right)^2 \right]^{1/2}, \\ d_{ij}^{(2)} &= \pm p.v. \left[\left(\frac{\omega}{V_j^{(2)}} \right)^2 - \left(k^{(2)} \right)^2 \right]^{1/2}, \quad (j = 1, 2, 3, 4). \end{aligned}$$

(3) In the poroelastic solid Ω_3 ($h < z < \infty$)

$$\begin{aligned} \varphi_j^{(3)} &= F_{ij}^{(3)} \exp(\vec{A}_{ij}^{(3)} \cdot \vec{r}) \exp\{i(\vec{P}_{ij}^{(3)} \cdot \vec{r} - \omega t)\}, \quad (j \\ &= 1, 2, 3, 4), \end{aligned} \tag{18}$$

where arbitrary constants $F_{ij}^{(3)}$, ($j = 1, 2, 3, 4$), represent the amplitudes of transmitted P_1, P_2, P_3, SV waves, respectively.

The propagation vectors $\vec{P}_{ij}^{(3)}$ and attenuation vectors $\vec{A}_{ij}^{(3)}$ are defined as

$$\begin{aligned} \vec{P}_{rj}^{(3)} &= k_R^{(3)} \hat{x} + d_{rjR}^{(3)} \hat{z}, & \vec{A}_{rj}^{(3)} &= -k_I^{(3)} \hat{x} - d_{rjI}^{(3)} \hat{z}, \\ d_{rj}^{(3)} &= \pm p.v. \left[\left(\frac{\omega}{V_j^{(3)}} \right)^2 - \left(k^{(3)} \right)^2 \right]^{1/2}, \quad (j = 1, 2, 3, 4). \end{aligned}$$

Sign of $d_{ij}^{(3)}$ is chosen to ensure the decay of the associated transmitted wave along the positive z -direction, i.e., a positive value for the imaginary part of $d_{ij}^{(3)}$. The subscripts t, r indicate the transmitted and reflected waves, respectively.

To satisfy the system of boundary conditions defined by (11), the potentials given by (15), (16), (17) and (18) are used to calculate the displacements and stresses in the media Ω_j , ($j = 1, 2, 3$). The continuity requirements along the interfaces $z = 0$ and $z = h$ are satisfied with the identical phase for all the waves on either side of the interfaces. This provides that Snell’s law for reflection/transmission phenomenon is considered. This translates further into the same wave number for all the waves across interfaces, i.e., $k = k^{(1)} = k^{(2)} = k^{(3)}$. Then, for an incident wave specified with V_0, θ_0, γ_0 and ω, k is calculated from (12). This k is used further to calculate $d_{rj}^{(m)}, d_{ij}^{(m)}$, ($m = 1, 2, 3$), for reflected and transmitted waves, respectively. Applying boundary conditions (11) and considering Snell’s law at the interfaces $z = 0$ and $z = h$, we get two systems of simultaneous linear equations (see Appendix 1). These two systems of equations are combined by using matrix notations of Carcione (2007,

Section 6.4) to relate the fields at $z = 0$ and $z = h$. Hence, these two systems are translated into a system of eight simultaneous linear equations given by

$$(\mathbf{M} - \mathbf{N} * \mathbf{O})\mathbf{Q} = \mathbf{R}, \tag{19}$$

where $\mathbf{Q} = [C_{r1}^{(1)}, C_{r2}^{(1)}, C_{r3}^{(1)}, C_{r4}^{(1)}, C_{t1}^{(3)}, C_{t2}^{(3)}, C_{t3}^{(3)}, C_{t4}^{(3)}]^T$, and $\mathbf{N} = \mathbf{T}(0) * \mathbf{T}(h)^{-1}$.

The matrices \mathbf{M}, \mathbf{O} and \mathbf{T} are given in Appendix 2. The matrix \mathbf{R} in the system (19) is written as follows.

- (1) For incident P -waves

$$\mathbf{R} = [-m_{1j}, m_{2j}, -m_{3j}, -m_{4j}, -m_{5j}, m_{6j}, m_{7j}, m_{8j}]^T, \quad (j = 1, 2, 3).$$
- (2) For incident SV -wave

$$\mathbf{R} = [m_{14}, -m_{24}, m_{34}, m_{44}, m_{54}, -m_{64}, -m_{74}, -m_{84}]^T.$$

7 Numerical results and discussion

7.1 Numerical example

The expressions for velocities, reflection and transmission coefficients involve a large number of parameters. Hence, to study the dependence of reflection and transmission coefficients on layer thickness, wave frequency, liquid saturation, capillary pressure of the porous layer, propagation and attenuation direction of the incident wave, we restrict our numerical work to a particular model. In this model, medium Ω_1 is taken to be Columbia fine sandy loam saturated by an air–water mixture, medium Ω_2 is taken to be sandstone saturated by water, and CO_2 , medium Ω_3 is taken to be Columbia fine sandy loam saturated by an oil–water mixture.

Following Lo et al. (2005), the values of elastic and dynamic constants chosen for Columbia fine sandy loam (medium Ω_1) saturated by an air–water mixture are as follows. The skeletal frame of sandstone with bulk modulus $K_0 = 8.33$ MPa, rigidity modulus $G = 3.83$ MPa and density $\rho_0 = 2650$ kg/m³ supports the porosity $f = 0.45$. The pore space is filled with air of bulk modulus $K_1 = 0.145$ MPa, density $\rho_1 = 1.1$ kg/m³ and viscosity $\eta_1 = 18 \times 10^{-6}$ Ns/m² mixed with water of bulk modulus $K_2 = 2.25$ GPa, density $\rho_2 = 997$ kg/m³ and viscosity $\eta_2 = 0.001$ Ns/m². The fitting parameters $n = 2.145, \chi = 0.5$ along with intrinsic permeability $\chi_0 = 5.3 \times 10^{-13}$ m² of composite. The value of $K_{\text{cap}} = 0.005K_2$ and $\sigma = 0.5$.

A reservoir rock (sandstone) saturated with water and CO_2 (medium Ω_2) is chosen for the numerical model of the poroelastic layer (Garg and Nayfeh 1986). The skeletal frame of sandstone with bulk modulus $K_0 = 12$ GPa, rigidity modulus $G = 9$ GPa and density $\rho_0 = 2650$ kg/m³ supports the porosity $f = 0.45$. The pore space is filled with

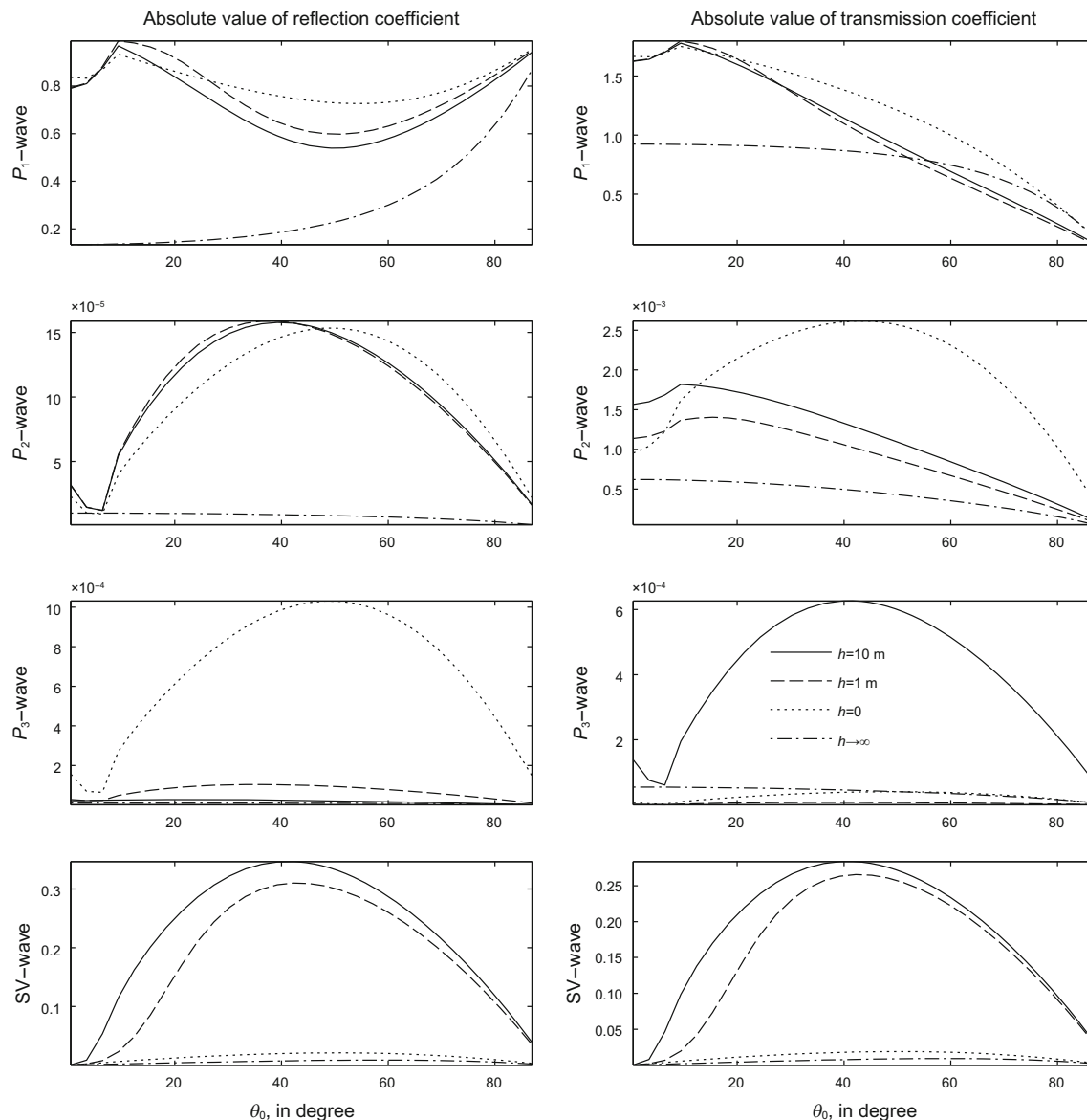


Fig. 2 Reflection and transmission coefficients as a function of incident direction (θ_0) for four different layer thickness: $h = 0, 1, 10$ m and $h \rightarrow \infty$; $\omega = 2\pi \times 100$ Hz; $\sigma = 0.2$; $K_{\text{cap}} = 0.005K_2$; incident P_1 wave

gas of bulk modulus $K_1 = 3.7$ MPa and density $\rho_1 = 103$ kg/m³ mixed with water of bulk modulus $K_2 = 2.25$ GPa and density $\rho_2 = 990$ kg/m³. Viscous dissipation in pores is defined with coefficient $d_1 = 0.04$ MPa s m⁻² for gas and $d_2 = 1$ MPa s m⁻² for water.

Following Lo et al. (2005), the values of elastic and dynamic constants chosen for Columbia fine sandy loam (medium Ω_3) saturated by an oil–water mixture are: the skeletal frame of sandstone with bulk modulus $K_0 = 8.33$ MPa, rigidity modulus $G = 3.85$ MPa and density $\rho_0 = 2650$ kg/m³ supports the porosity $f = 0.45$. The pore space is filled with oil of bulk modulus $K_1 = 0.57$ GPa, density $\rho_1 = 762$ kg/m³ and viscosity $\eta_1 = 0.00144$ Ns/m²

mixed with water of bulk modulus $K_2 = 2.25$ GPa, density $\rho_2 = 997$ kg/m³ and viscosity $\eta_2 = 0.001$ Ns/m². The fitting parameters are $n = 2.037$, $\chi = 0.5$ along with intrinsic permeability $\chi_0 = 8 \times 10^{-13}$ m² of composite. The value of $K_{\text{cap}} = 0.005K_2$ and $\sigma = 0.5$.

7.2 Numerical discussion

The reflection and transmission coefficients defined in Sect. 6 are calculated for incident direction $\theta_0 \in (0, 90^\circ)$. In this article, the incidence of two main waves (i.e., P_1 and SV) is considered. The variations of reflection and transmission coefficients with incident direction (θ_0) are

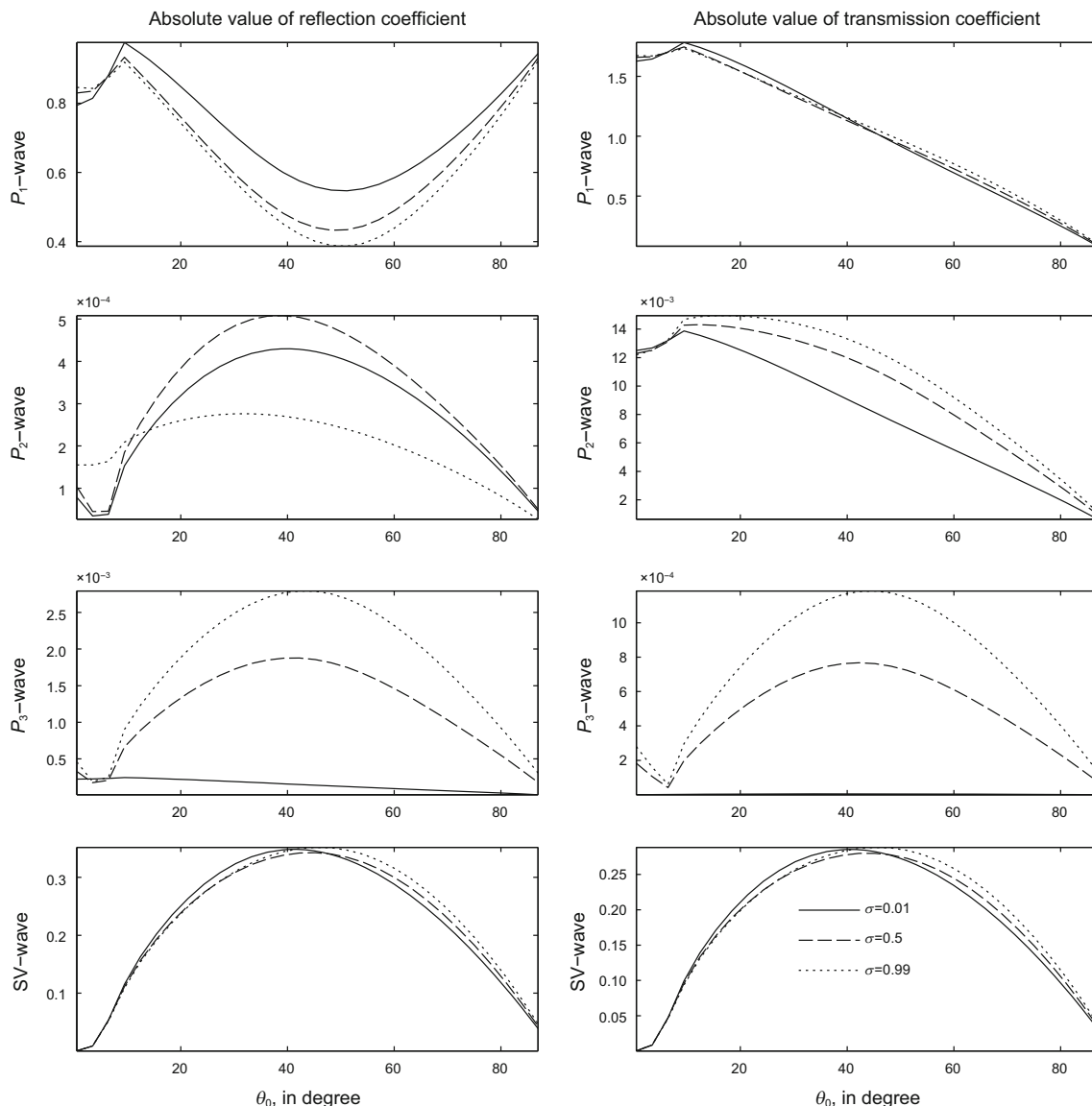


Fig. 3 Reflection and transmission coefficients as a function of incident direction (θ_0) for three different liquid saturations: $\sigma = 0.01, 0.5, 0.99$; $\omega = 2\pi \times 1000\text{Hz}$; $h = 1\text{m}$; $K_{\text{cap}} = 0.02K_2$; incident P_1 wave

shown in Figs. 2–6 (for incident P_1 wave) and in Figs. 7–11 (for incident SV wave). The detailed discussion on figures is as follows.

Figure 2 displays the variation of reflection and transmission coefficients as a function of incident direction (θ_0) for four different values of h : 0, 1, 10 m and $h \rightarrow \infty$. The reflected and transmitted SV waves get stronger with an increase in layer thickness. It is clear that at normal incidence reflected and transmitted SV waves do not survive quantitatively for any value of layer thickness (h). The transmission coefficients of P_1, P_2, P_3 waves behave differently to reflection coefficients in regards to layer

thickness. A critical angle is observed between 8° and 15° . In both cases (i.e., $h = 0$ and $h \rightarrow \infty$), the poroelastic layer is eliminated from the system and represents the reflection and transmission of waves at the boundary between two dissimilar poroelastic solids saturated with two immiscible fluids. In case of $h = 0$, the variations in reflection and transmission coefficients with incident direction are different from that in the case of $h \rightarrow \infty$. This variation in reflection and transmission coefficients occurs due to the difference in the numerical values of elastic/dynamical constants of the two media. The effect of the saturating fluid on the variation of reflection and transmission

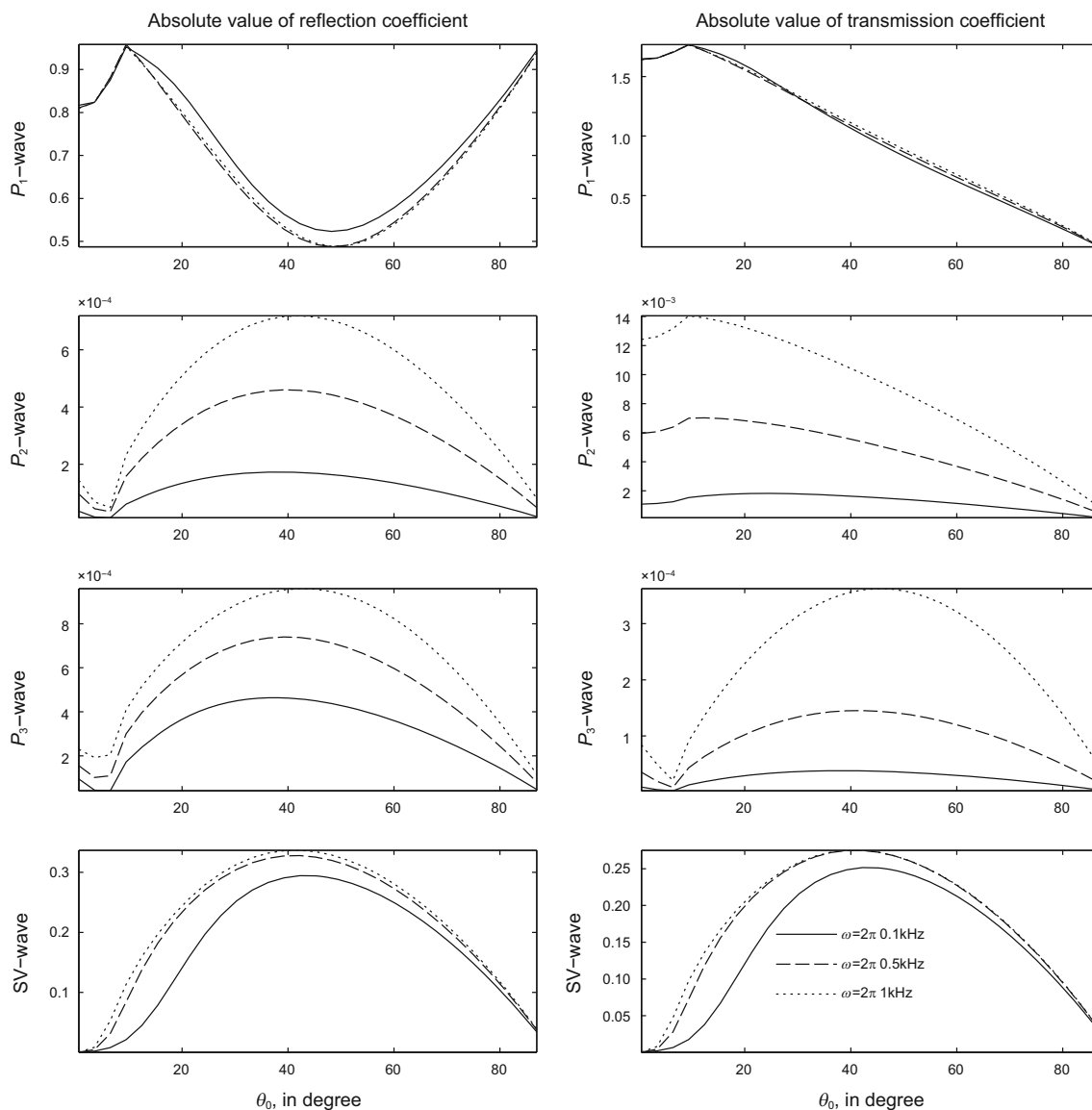


Fig. 4 Reflection and transmission coefficients as a function of incident direction (θ_0) for three different frequencies: $\omega = 2\pi \times 0.1\text{kHz}$, $2\pi \times 0.5\text{kHz}$, $2\pi \times 1\text{kHz}$; $h = 1\text{m}$; $\sigma = 0.5$; $K_{\text{cap}} = 0.005K_2$; incident P_1 wave

coefficients is shown in Fig. 3. It is observed that the transmission coefficients of P_3 and SV waves behave almost like reflection coefficients, for any value of σ . However, with the change in σ , the transmission coefficients of P_1 and P_2 waves behave opposite to reflection coefficients. The effect of wave frequency on reflection and transmission coefficients is displayed in Fig. 4. It is noticed that the reflection and transmission coefficients of P_2 , P_3 and SV waves increase with an increase in wave frequency ω . The effect of frequency on the transmission coefficient of the P_1 wave is insignificant. However, beyond 10° incidence, the reflection coefficient of the P_1 wave decreases with an increase in frequency. Further, the

behavior of the transmission coefficient of P_1 is opposite to the corresponding reflection coefficient for $\theta_0 \in (50^\circ, 90^\circ)$. The effect of capillary pressure on the reflection and transmission coefficients is displayed in Fig. 5. For $\theta_0 \in (0, 90^\circ)$, the transmission coefficients of P_3 and SV waves behave like their corresponding reflection coefficients. However, the transmission coefficients of P_1 and P_2 waves behave opposite to the reflection coefficients with the change in capillary pressure. The effect of viscosity of pore fluids on reflection and transmission coefficients is shown in Fig. 6. The viscosity of pore fluids may have considerable effect on all the reflected and transmitted waves for $\theta_0 \in (20^\circ, 85^\circ)$ except for the transmitted P_1

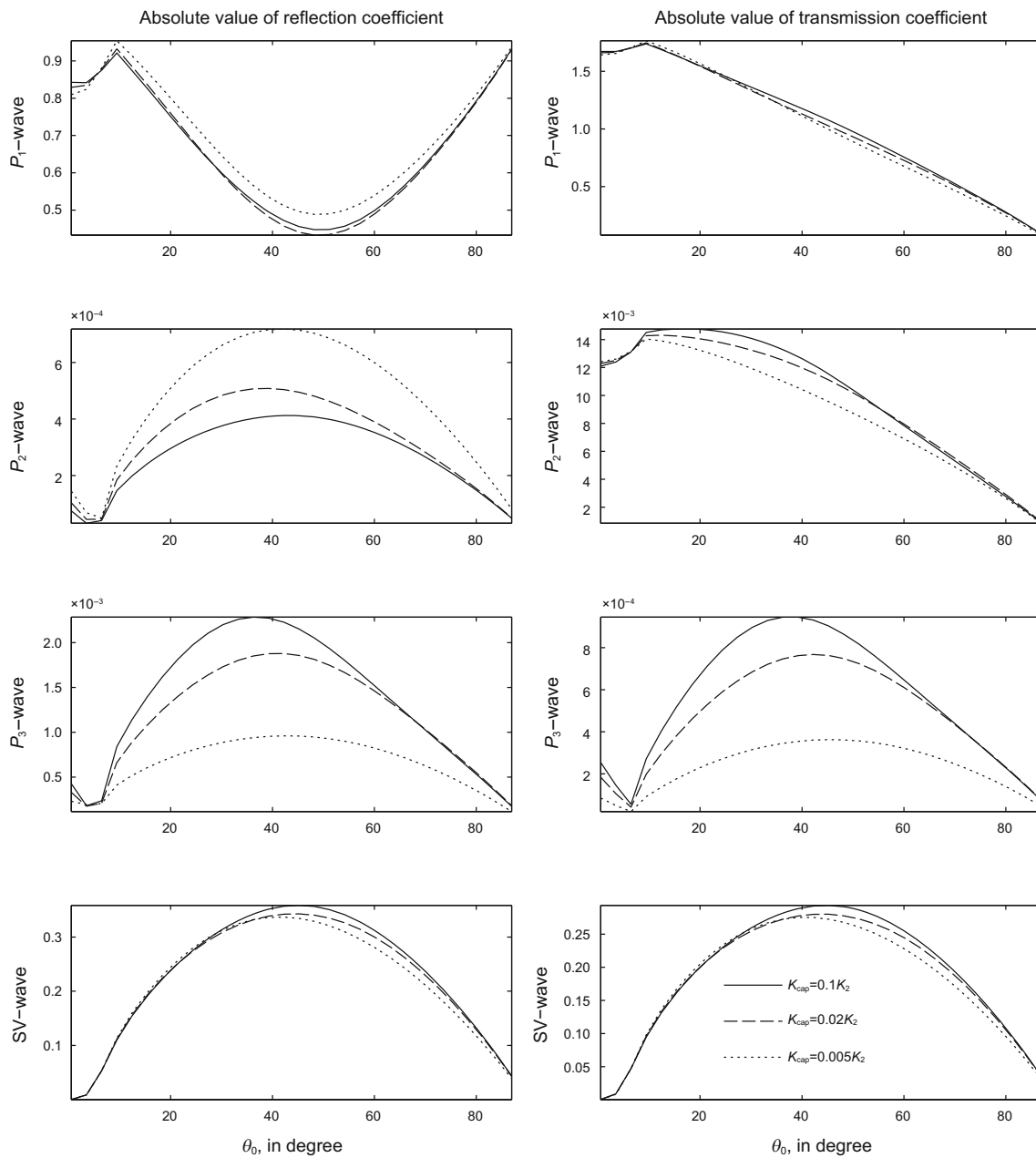


Fig. 5 Reflection and transmission coefficients as a function of incident direction (θ_0) for three different values of capillary pressure: $K_{cap} = 0.1K_2, 0.02K_2, 0.005K_2$; $\omega = 2\pi \times 1000\text{Hz}$; $\sigma = 0.5$; $h = 1\text{m}$; incident P_1 wave

wave. The reflection coefficient of the P_1 wave increases due to the presence of viscosity in pore fluids, while all the other reflection and transmission coefficients decrease due to the presence of viscosity in pore fluids.

For the incidence of the SV wave, the reflection and transmission coefficients as a function of incident direction (θ_0) are shown in Fig. 7 for four different values of h : 0, 1, 10 m and $h \rightarrow \infty$. In Fig. 7, a significant effect of variations in layer thickness is observed on the reflection and transmission coefficients. It is clear that at normal incidence only reflected SV waves survive quantitatively for

any value of layer thickness (h). In the absence of a sandwiched layer (i.e., $h = 0$), a critical angle is not observed for both reflected and transmitted SV waves, while critical angles are observed for all the other reflected and transmitted waves. The effect of saturation (σ) on reflection and transmission coefficients is shown in Fig. 8. A significant effect of saturation is observed on the reflection and transmission coefficients of P_2 and P_3 waves, while P_1 and SV waves are only slightly influenced by a change in liquid saturation. The transmission coefficients of P_2 waves behave nearly opposite to their corresponding

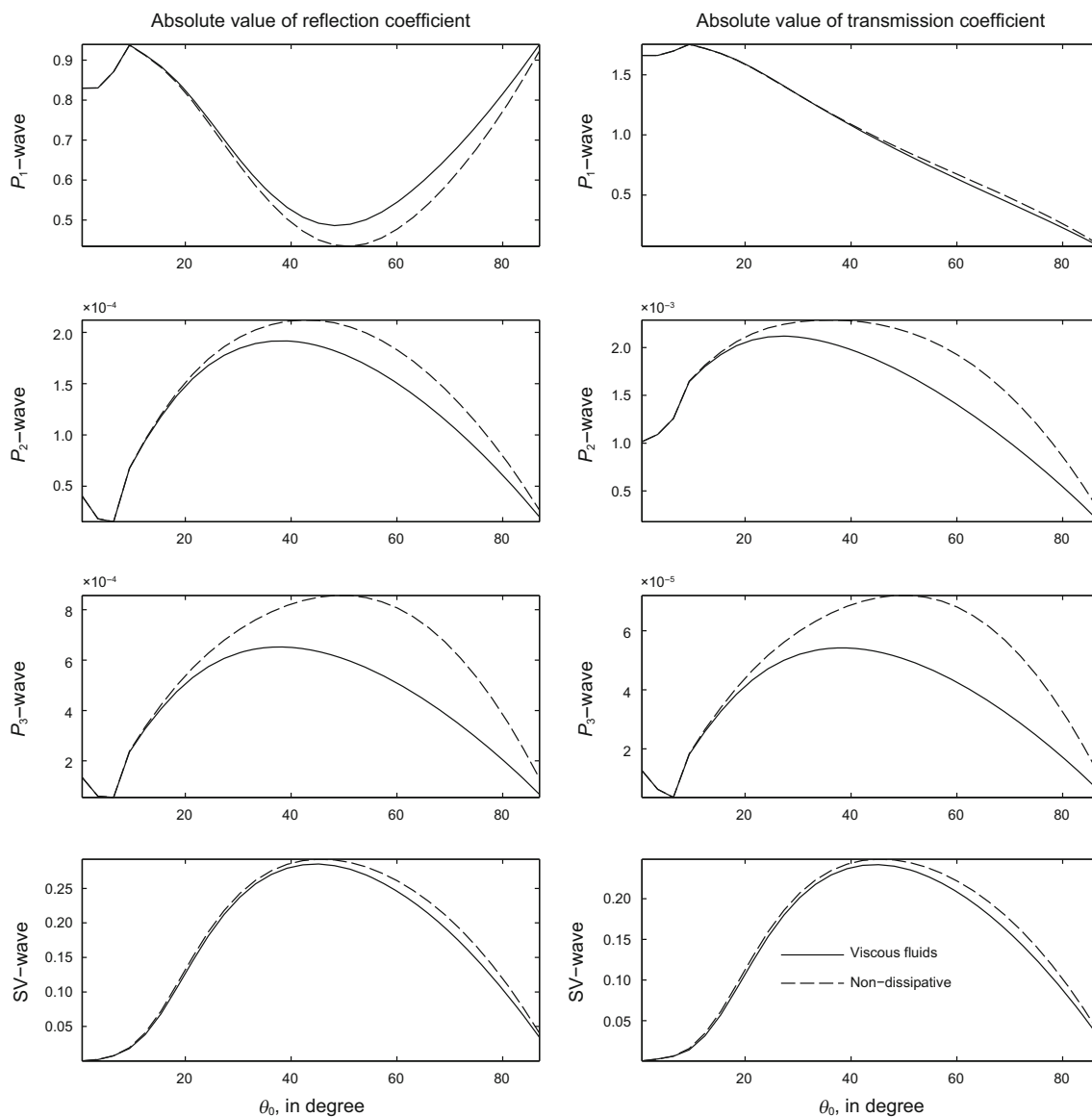


Fig. 6 Effect of viscosity of pore fluids on reflection and transmission coefficients; $h = 1\text{m}$; $K_{\text{cap}} = 0.005K_2$; $\omega = 2\pi \times 100\text{Hz}$; $\sigma = 0.8$; incident P_1 wave

reflection coefficient with respect to saturation. In Fig. 9, a significant effect of variations in frequency is visible on all the reflected and transmitted waves. Hence, all the waves are dispersive in nature. In Fig. 10, a small effect of capillary pressure is observed on the two main waves (i.e., P_1 , SV), but a significant effect of capillary pressure is observed on the two slower waves (i.e., P_2 , P_3). The effect of viscosity of pore fluids on reflection and transmission coefficients is shown in Fig. 11. Similar to the case of incident P_1 wave, the presence of viscosity in pore fluids may have considerable effect on the reflection and transmission coefficients for $\theta_0 \in (20^\circ, 80^\circ)$. The variational pattern of transmission coefficients is nearly similar to reflection coefficients except for the SV wave.

8 Conclusions

In the present study, a theoretical procedure is used to analyze the effects of layer thickness, liquid saturation, capillary pressure of the porous layer, incident direction and wave frequency on the reflection and transmission characteristics. This mathematical model can be used in many practical applications such as to predict the seismic response of fractures in sandstones. Some interesting consequences of the present study are explained as follows.

- (1) At the normal incidence of P_1 wave, reflected and transmitted SV waves do not survive quantitatively, while at the normal incidence of SV wave, only transmitted SV waves survive.

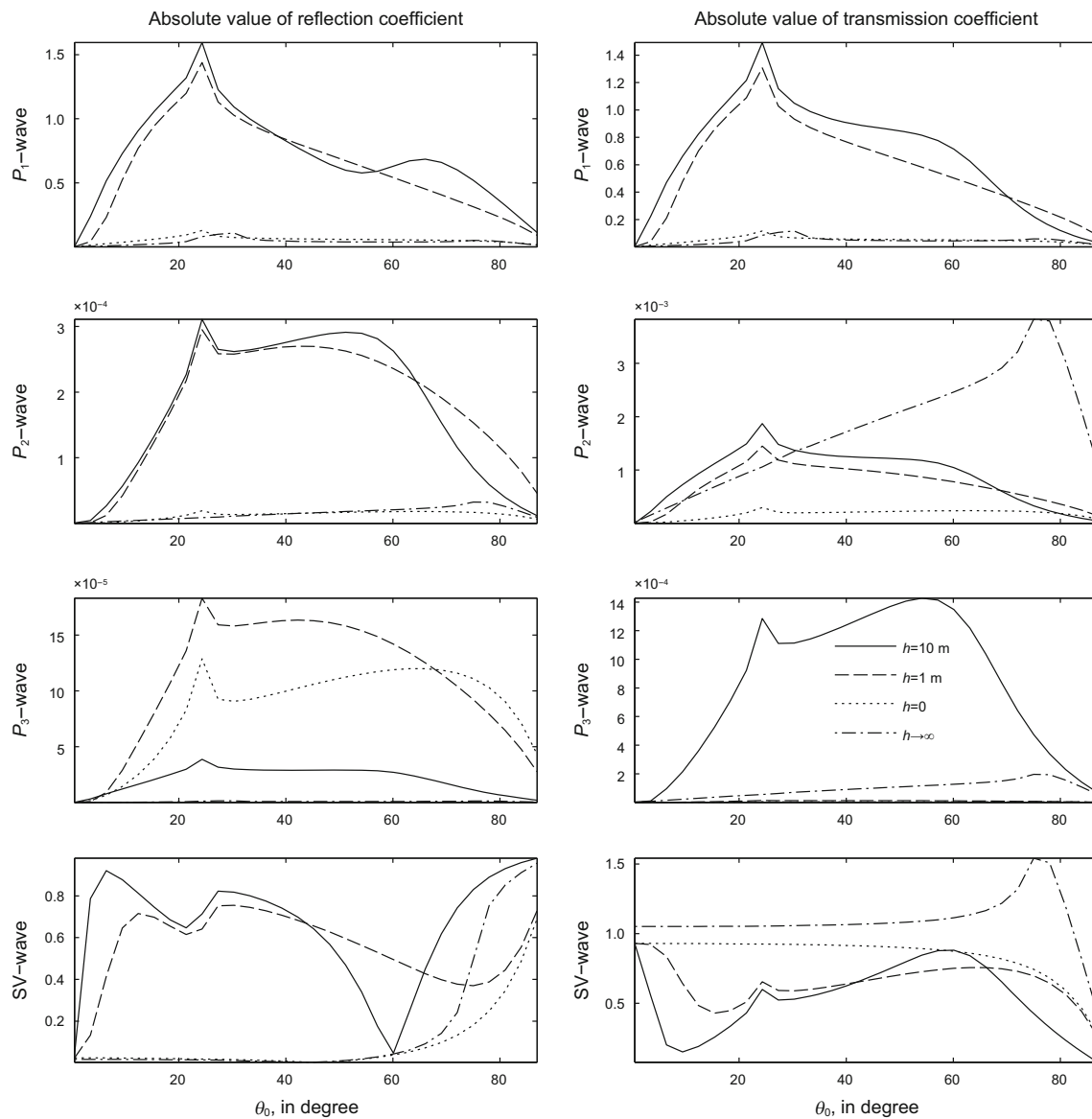


Fig. 7 Same as Fig. 2 but for incident SV wave

- (2) All the reflected and transmitted waves are strongly influenced by variations in frequency for both incidence (i.e., P_1 and SV). Therefore, all the reflected and transmitted waves are frequency dependent in nature.
- (3) For the incidence of SV wave, in the absence of a sandwiched layer (i.e., $h = 0$ and $h \rightarrow \infty$), a critical angle is not observed for either reflected or transmitted SV waves.
- (4) All the reflected and transmitted waves are significantly influenced by the presence of viscosity in pore fluids for both incidences.
- (5) For both incidences, all reflected and transmitted waves are strongly associated with layer thickness,

liquid saturation, capillary pressure of the sandwiched layer and incident direction.

The study of reservoir characteristics such as layer thickness, capillary pressure and saturation through seismic (reflection and transmission) methods is helpful in detecting hydrocarbons and minerals present beneath the Earth’s surface. Hence, the various issues resolved in this study are relevant to many of the practical problems of hydrology, geophysics, petroleum engineering and seismology.

Open Access This article is distributed under the terms of the Creative Commons Attribution 4.0 International License (<http://creativecommons.org/licenses/by/4.0/>), which permits unrestricted use, distribution, and reproduction in any medium, provided you give appropriate credit to the original author(s) and the source, provide a link to the Creative Commons license, and indicate if changes were made.

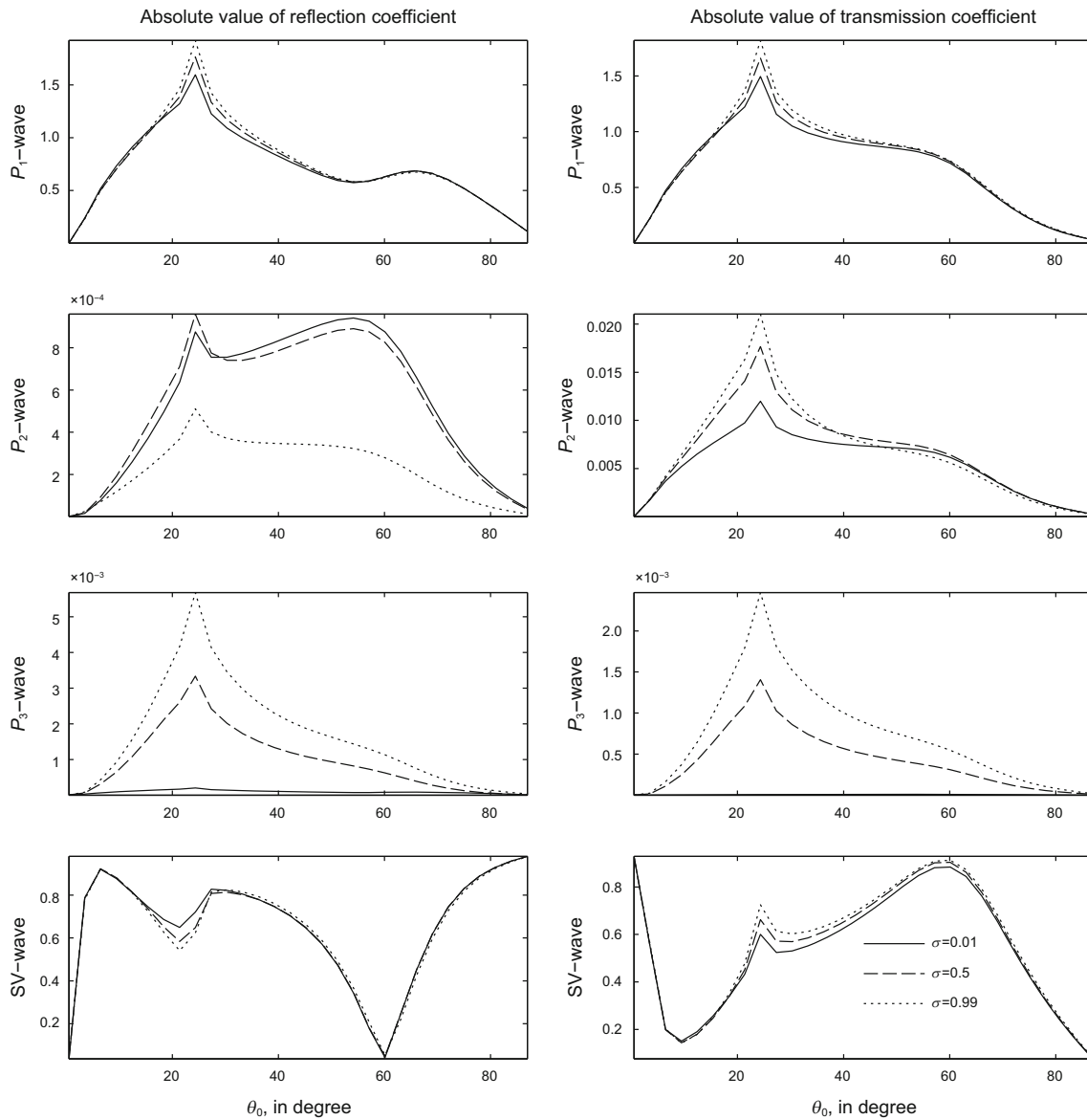


Fig. 8 Same as Fig. 3 but for incident SV wave

Appendix 1: Linear systems

The first system of simultaneous linear equations at the interface $z = 0$ is given by

$$\sum_{j=1}^4 x_{i,j} C_{rj}^{(1)} + \sum_{j=5}^8 x_{i,j} C_{rl}^{(2)} + \sum_{j=9}^{12} x_{i,j} C_{rq}^{(2)} = b_i, \quad l = j - 4,$$

$$q = j - 8, \quad i = 1, 2, 3, 4, 5, 6, 7, 8. \tag{20}$$

where

$$x_{1,j} = - [\alpha_j^{(1)} + (\alpha_j^{(1)} + 2G^{(1)})(d_{rj}^{(1)}/k)^2],$$

$$x_{1,4} = 2G^{(1)}(d_{r4}^{(1)}/k), \quad x_{2,j} = 2G^{(1)}(d_{rj}^{(1)}/k),$$

$$x_{2,4} = G^{(1)}((d_{r4}^{(1)}/k)^2 - 1), \quad x_{3,j} = -\beta_j^{(1)}(1 + (d_{rj}^{(1)}/k)^2),$$

$$x_{3,4} = 0, \quad x_{4,j} = -\gamma_j^{(1)}(1 + (d_{rj}^{(1)}/k)^2), \quad x_{4,4} = 0.$$

For $(j = 5, 6, 7; l = j - 4)$, we have

$$x_{5,j} = 1, \quad x_{5,4} = d_{r4}^{(1)}/k, \quad x_{6,j} = -d_{rj}^{(1)}/k, \quad x_{6,4} = 1,$$

$$x_{7,j} = -\mu_j^{(1)}(d_{rj}^{(1)}/k), \quad x_{7,4} = \Gamma_1^{(1)}, \quad x_{8,j} = -\gamma_j^{(1)}(d_{rj}^{(1)}/k),$$

$$x_{8,4} = \Gamma_2^{(1)}.$$

For $(j = 5, 6, 7; l = j - 4)$, we have

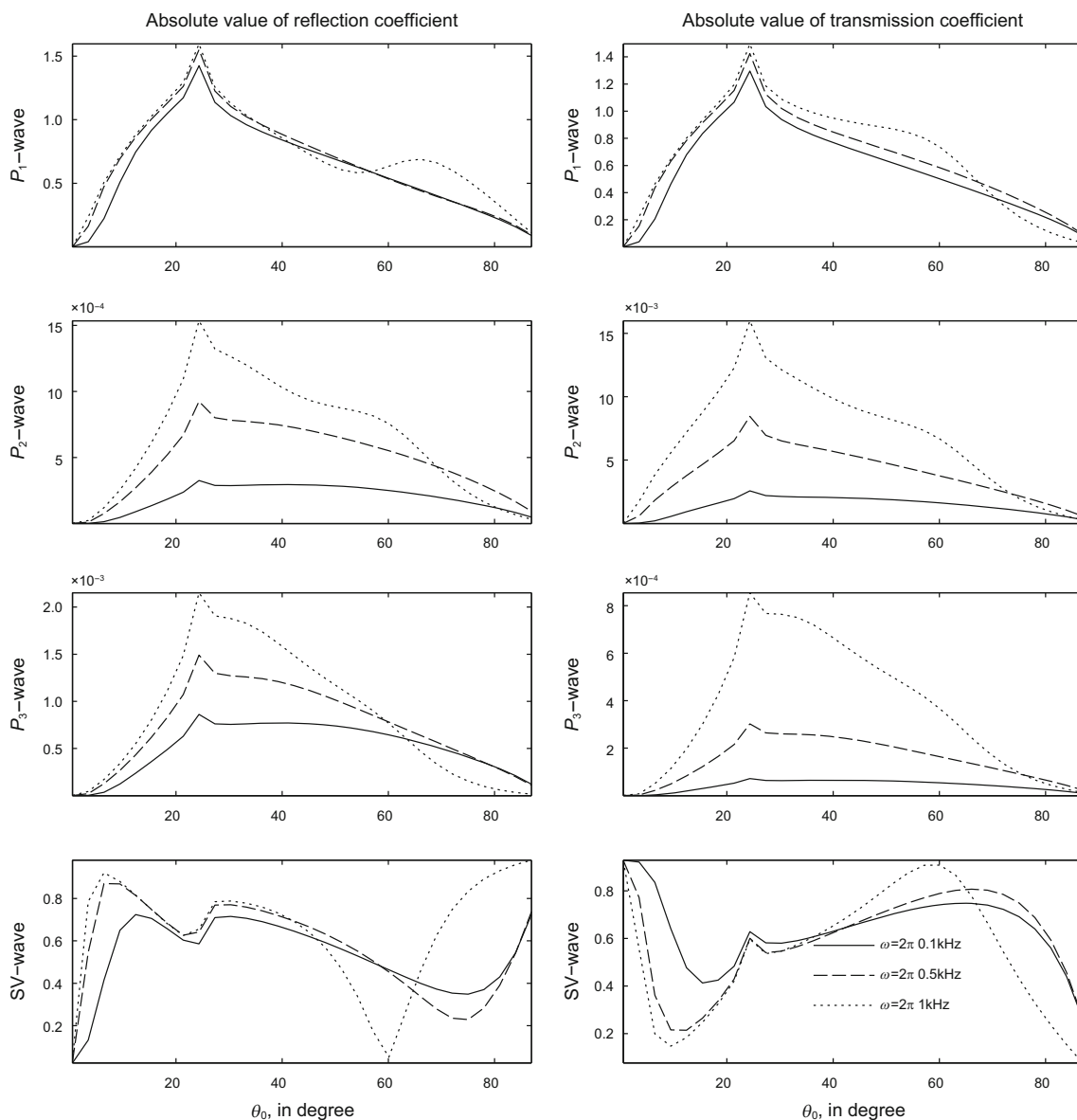


Fig. 9 Same as Fig. 4 but for incident SV wave

$$\begin{aligned}
 x_{1,j} &= [\alpha_l^{(2)} + (\alpha_l^{(2)} + 2G^{(2)})(d_{il}^{(2)}/k)^2], \quad x_{1,8} = 2G^{(2)}(d_{i4}^{(2)}/k), \\
 x_{2,j} &= 2G^{(2)}(d_{il}^{(2)}/k), \quad x_{2,8} = -G^{(2)}((d_{i4}^{(2)}/k)^2 - 1), \\
 x_{3,j} &= \beta_l^{(2)}(1 + (d_{il}^{(2)}/k)^2), \quad x_{3,8} = 0, \\
 x_{4,j} &= \gamma_l^{(2)}(1 + (d_{il}^{(2)}/k)^2), \quad x_{4,8} = 0, \\
 x_{5,j} &= -1, \quad x_{5,8} = d_{i4}^{(2)}/k, \quad x_{6,j} = -d_{il}^{(2)}/k, \quad x_{6,8} = -1, \\
 x_{7,j} &= -\mu_l^{(2)}(d_{il}^{(2)}/k), \quad x_{7,8} = -\Gamma_1^{(2)}, \\
 x_{8,j} &= -\gamma_l^{(2)}(d_{il}^{(2)}/k), \quad x_{8,4} = -\Gamma_2^{(2)}.
 \end{aligned}$$

For $(j = 9, 10, 11; q = j - 8)$, we have

$$\begin{aligned}
 x_{1,j} &= [\alpha_q^{(2)} + (\alpha_q^{(2)} + 2G^{(2)})(d_{rq}^{(2)}/k)^2], \\
 x_{1,12} &= 2G^{(2)}(d_{r4}^{(2)}/k), \quad x_{2,j} = -2G^{(2)}(d_{rq}^{(2)}/k), \\
 x_{2,12} &= -G^{(2)}((d_{r4}^{(2)}/k)^2 - 1), \quad x_{3,j} = \beta_q^{(2)}(1 + (d_{rq}^{(2)}/k)^2), \\
 x_{3,12} &= 0, \quad x_{4,j} = \gamma_q^{(2)}(1 + (d_{rq}^{(2)}/k)^2), \quad x_{4,12} = 0, \\
 x_{5,j} &= -1, \quad x_{5,12} = -d_{r4}^{(2)}/k, \quad x_{6,j} = d_{rq}^{(2)}/k, \quad x_{6,12} = -1, \\
 x_{7,j} &= \mu_q^{(2)}(d_{rq}^{(2)}/k), \quad x_{7,12} = -\Gamma_1^{(2)}, \quad x_{8,j} = \gamma_q^{(2)}(d_{rq}^{(2)}/k), \\
 x_{8,12} &= -\Gamma_2^{(2)}.
 \end{aligned}$$

The second system of simultaneous linear equations at the interface $z = h$, is given by

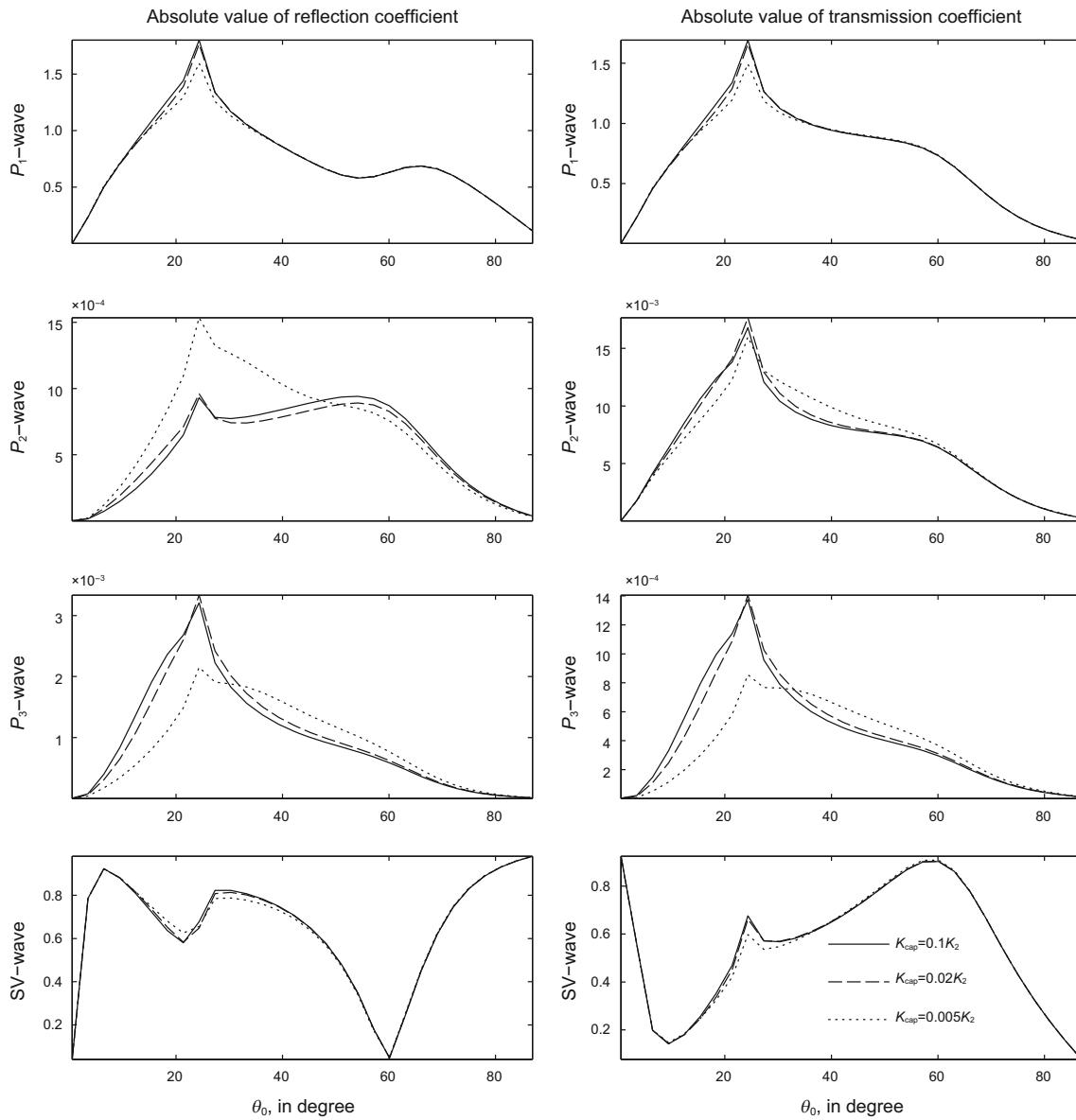


Fig. 10 Same as Fig. 5 but for incident SV wave

$$\sum_{j=1}^4 y_{i,j} e^{i d_j^{(2)} h} C_{ij}^{(2)} + \sum_{j=5}^8 y_{i,j} e^{-i d_j^{(2)} h} C_{rq}^{(2)} = \sum_{j=1}^4 z_{i,j} e^{i d_j^{(2)} h} C_{ij}^{(3)},$$

$$q = j - 8, \quad i = 1, 2, 3, 4, 5, 6, 7, 8. \tag{21}$$

For $(j = 1, 2, 3)$, we have

$$y_{1,j} = - [\alpha_j^{(2)} + (\alpha_j^{(2)} + 2G^{(2)})(d_{ij}^{(2)}/k)^2],$$

$$y_{1,4} = - 2G^{(2)}(d_{14}^{(2)}/k),$$

$$y_{2,j} = -2G^{(2)}(d_{ij}^{(2)}/k), \quad y_{2,4} = G^{(2)}((d_{14}^{(2)}/k)^2 - 1),$$

$$y_{3,j} = - \beta_j^{(2)}(1 + (d_{ij}^{(2)}/k)^2),$$

$$y_{3,4} = 0, \quad y_{4,j} = - \gamma_j^{(2)}(1 + (d_{ij}^{(2)}/k)^2), \quad y_{4,4} = 0,$$

$$y_{5,j} = 1, \quad y_{5,4} = - d_{14}^{(2)}/k, \quad y_{6,j} = d_{ij}^{(2)}/k, \quad y_{6,4} = 1,$$

$$y_{7,j} = \mu_j^{(2)}(d_{ij}^{(2)}/k), \quad y_{7,4} = \Gamma_1^{(2)}, \quad y_{8,j} = \gamma_j^{(2)}(d_{ij}^{(2)}/k),$$

$$y_{8,4} = \Gamma_2^{(2)}.$$

For $(j = 5, 6, 7; q = j - 4)$, we have

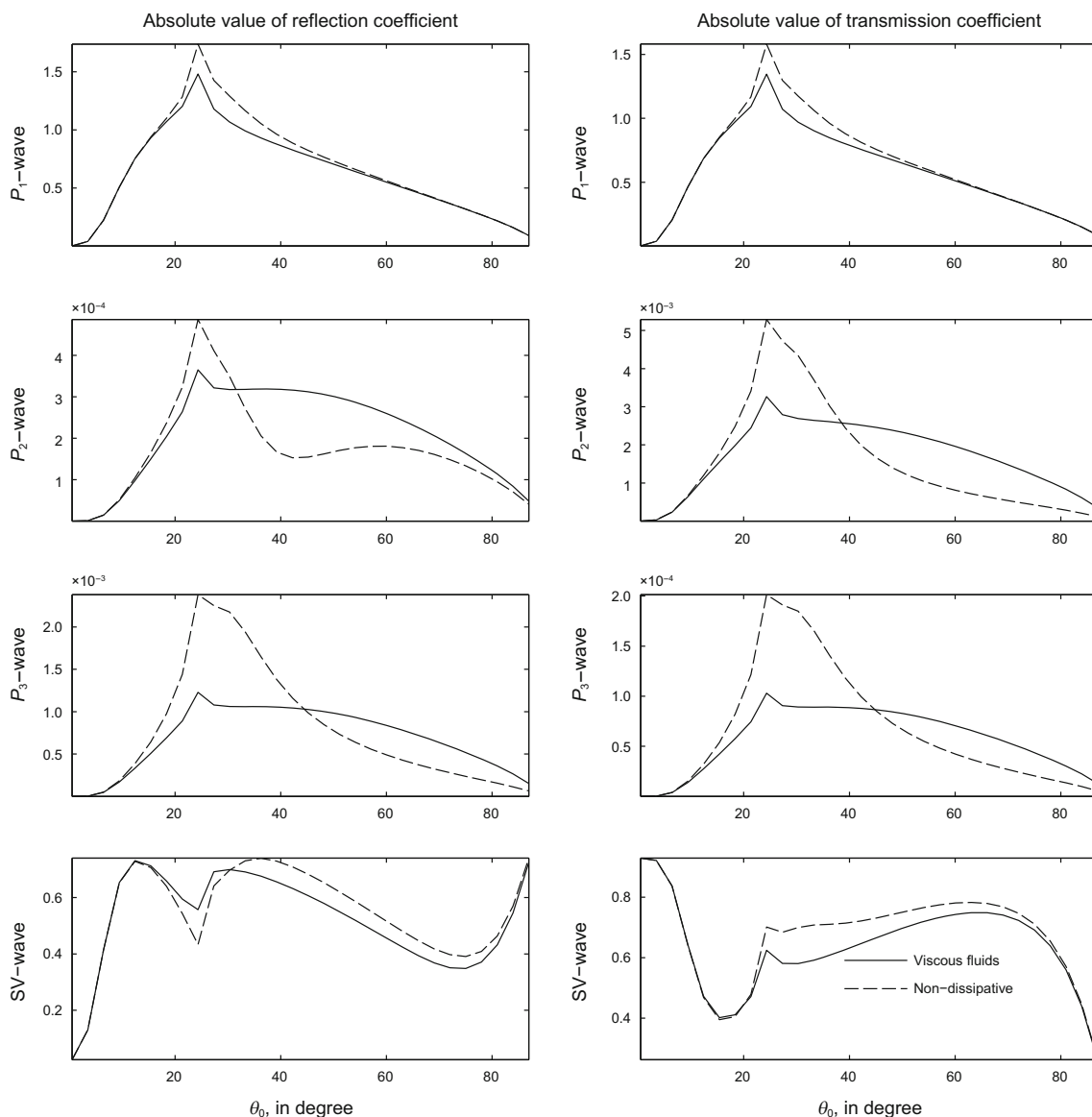


Fig. 11 Same as Fig. 6 but for incident SV wave

$$\begin{aligned}
 y_{1,j} &= -[\alpha_q^{(2)} + (\alpha_q^{(2)} + 2G^{(2)})(d_{rq}^{(2)}/k)^2], \\
 y_{1,8} &= 2G^{(2)}(d_{r4}^{(2)}/k), \quad y_{2,j} = 2G^{(2)}(d_{rq}^{(2)}/k), \\
 y_{2,8} &= -G^{(2)}((d_{r4}^{(2)}/k)^2 - 1), \quad y_{3,j} = -\beta_q^{(2)}(1 + (d_{rq}^{(2)}/k)^2), \\
 y_{3,8} &= 0, \quad y_{4,j} = -\gamma_q^{(2)}(1 + (d_{rq}^{(2)}/k)^2), \quad y_{4,8} = 0, \\
 y_{5,j} &= 1, \quad y_{5,8} = d_{r4}^{(2)}/k, \quad y_{6,j} = -d_{rq}^{(2)}/k, \quad y_{6,8} = 1, \\
 y_{7,j} &= -\mu_q^{(2)}(d_{rq}^{(2)}/k), \quad y_{7,8} = \Gamma_1^{(2)}, \\
 y_{8,j} &= -\gamma_q^{(2)}(d_{rq}^{(2)}/k), \quad y_{8,4} = \Gamma_2^{(2)}.
 \end{aligned}$$

For $(j = 1, 2, 3)$, we have

$$\begin{aligned}
 z_{1,j} &= -[\alpha_j^{(3)} + (\alpha_j^{(3)} + 2G^{(3)})(d_{ij}^{(3)}/k)^2]e^{id_{ij}^{(3)}h}, \\
 z_{1,4} &= -2G^{(3)}(d_{i4}^{(3)}/k)e^{id_{i4}^{(3)}h}, \\
 z_{2,j} &= -2G^{(3)}(d_{ij}^{(3)}/k)e^{id_{ij}^{(3)}h}, \\
 z_{2,4} &= G^{(3)}((d_{i4}^{(3)}/k)^2 - 1)e^{id_{i4}^{(3)}h}, \\
 z_{3,j} &= -\beta_j^{(3)}(1 + (d_{ij}^{(3)}/k)^2)e^{id_{ij}^{(3)}h}, \quad z_{3,4} = 0, \\
 z_{4,j} &= -\gamma_j^{(3)}(1 + (d_{ij}^{(3)}/k)^2)e^{id_{ij}^{(3)}h}, \quad z_{4,4} = 0, \\
 z_{5,j} &= e^{id_{ij}^{(3)}h}, \quad z_{5,4} = -(d_{i4}^{(3)}/k)e^{id_{i4}^{(3)}h}, \\
 z_{6,j} &= (d_{ij}^{(3)}/k)e^{id_{ij}^{(3)}h}, \quad z_{6,4} = e^{id_{i4}^{(3)}h},
 \end{aligned}$$

$$z_{7,j} = \mu_j^{(3)}(d_{ij}^{(3)}/k)e^{id_{ij}^{(3)}h}, \quad z_{7,4} = \Gamma_1^{(3)}e^{id_{i4}^{(3)}h},$$

$$z_{8,j} = \gamma_j^{(3)}(d_{ij}^{(3)}/k)e^{id_{ij}^{(3)}h}, \quad z_{8,4} = \Gamma_2^{(3)}e^{id_{i4}^{(3)}h}.$$

Appendix 2: Linear systems

The final system of linear equations. The matrices given in system (19) are defined as

$$M = \begin{bmatrix} x_{1,1} & x_{1,2} & x_{1,3} & x_{1,4} & 0 & 0 & 0 & 0 \\ x_{2,1} & x_{2,2} & x_{2,3} & x_{2,4} & 0 & 0 & 0 & 0 \\ x_{3,1} & x_{3,2} & x_{3,3} & x_{3,4} & 0 & 0 & 0 & 0 \\ x_{4,1} & x_{4,2} & x_{4,3} & x_{4,4} & 0 & 0 & 0 & 0 \\ x_{5,1} & x_{5,2} & x_{5,3} & x_{5,4} & 0 & 0 & 0 & 0 \\ x_{6,1} & x_{6,2} & x_{6,3} & x_{6,4} & 0 & 0 & 0 & 0 \\ x_{7,1} & x_{7,2} & x_{7,3} & x_{7,4} & 0 & 0 & 0 & 0 \\ x_{8,1} & x_{8,2} & x_{8,3} & x_{8,4} & 0 & 0 & 0 & 0 \end{bmatrix}$$

and

$$O = \begin{bmatrix} 0 & 0 & 0 & 0 & z_{1,1} & z_{1,2} & z_{1,3} & z_{1,4} \\ 0 & 0 & 0 & 0 & z_{2,1} & z_{2,2} & z_{2,3} & z_{2,4} \\ 0 & 0 & 0 & 0 & z_{3,1} & z_{3,2} & z_{3,3} & z_{3,4} \\ 0 & 0 & 0 & 0 & z_{4,1} & z_{4,2} & z_{4,3} & z_{4,4} \\ 0 & 0 & 0 & 0 & z_{5,1} & z_{5,2} & z_{5,3} & z_{5,4} \\ 0 & 0 & 0 & 0 & z_{6,1} & z_{6,2} & z_{6,3} & z_{6,4} \\ 0 & 0 & 0 & 0 & z_{7,1} & z_{7,2} & z_{7,3} & z_{7,4} \\ 0 & 0 & 0 & 0 & z_{8,1} & z_{8,2} & z_{8,3} & z_{8,4} \end{bmatrix}$$

Finally, $N = T(0) * [T(h)]^{-1}$ and $T(z) = S_1 * S_2(z)$ being

$$S_1 = \begin{bmatrix} y_{1,1} & y_{1,2} & y_{1,3} & y_{1,4} & y_{1,5} & y_{1,6} & y_{1,7} & y_{1,8} \\ y_{2,1} & y_{2,2} & y_{2,3} & y_{2,4} & y_{2,5} & y_{2,6} & y_{2,7} & y_{2,8} \\ y_{3,1} & y_{3,2} & y_{3,3} & y_{3,4} & y_{3,5} & y_{3,6} & y_{3,7} & y_{3,8} \\ y_{4,1} & y_{4,2} & y_{4,3} & y_{4,4} & y_{4,5} & y_{4,6} & y_{4,7} & y_{4,8} \\ y_{5,1} & y_{5,2} & y_{5,3} & y_{5,4} & y_{5,5} & y_{5,6} & y_{5,7} & y_{5,8} \\ y_{6,1} & y_{6,2} & y_{6,3} & y_{6,4} & y_{6,5} & y_{6,6} & y_{6,7} & y_{6,8} \\ y_{7,1} & y_{7,2} & y_{7,3} & y_{7,4} & y_{7,5} & y_{7,6} & y_{7,7} & y_{7,8} \\ y_{8,1} & y_{8,2} & y_{8,3} & y_{8,4} & y_{8,5} & y_{8,6} & y_{8,7} & y_{8,8} \end{bmatrix}$$

and

$$S_2 = \begin{bmatrix} e^{id_{1z}} & 0 & 0 & 0 & 0 & 0 & 0 & 0 \\ 0 & e^{id_{2z}} & 0 & 0 & 0 & 0 & 0 & 0 \\ 0 & 0 & e^{id_{3z}} & 0 & 0 & 0 & 0 & 0 \\ 0 & 0 & 0 & e^{id_{4z}} & 0 & 0 & 0 & 0 \\ 0 & 0 & 0 & 0 & e^{-id_{1z}} & 0 & 0 & 0 \\ 0 & 0 & 0 & 0 & 0 & e^{-id_{2z}} & 0 & 0 \\ 0 & 0 & 0 & 0 & 0 & 0 & e^{-id_{3z}} & 0 \\ 0 & 0 & 0 & 0 & 0 & 0 & 0 & e^{-id_{4z}} \end{bmatrix}$$

References

Ainslie MA. Reflection and transmission coefficients for a layered fluid sediment overlying a uniform solid substrate. *J Acoust Soc Am.* 1996;99(2):893–902. doi:10.1121/1.414663.

Arora A, Tomar SK. Elastic waves at porous/porous elastic half-spaces saturated by two immiscible fluids. *J Porous Media.* 2007;10(8):751–68. doi:10.1615/JPorMedia.v10.i8.20.

Bai R, Tinel A, Alem A, Franklin H, Wang H. Ultrasonic characterization of water saturated double porosity media. *Phys Proced.* 2015;70:114–7. doi:10.1016/j.phpro.2015.08.055.

Bai R, Tinel A, Alem A, Franklin H, Wang H. Estimating frame bulk and shear moduli of two double porosity layers by ultrasound transmission. *Ultrasonics.* 2016;70:211–20. doi:10.1016/j.ultras.2016.05.004.

Borcherdt RD. Reflection-refraction of general P and type-I S waves in elastic and anelastic solids. *Geophys J R Astron Soc.* 1982;70(3):621–38. doi:10.1111/j.1365-246X.1982.tb05976.x.

Brekhovskikh LM. *Waves in layered media.* New York: Academic Press Inc; 1960. p. 45.

Carcione JM. Amplitude variations with offset of pressure-seal reflections. *Geophysics.* 2001;66(1):283–93. doi:10.1190/1.1444907.

Carcione JM. *Wave field in real media: wave propagation in anisotropic, anelastic, porous and electromagnetic media.* Amsterdam: Pergamon; 2007.

Carcione JM. *Wave field in real media: wave propagation in anisotropic, anelastic, porous and electromagnetic media.* Handbook of geophysical exploration. Amsterdam: Elsevier; 2014.

Cerveny V, Vanek J. Reflection and transmission coefficients for transition layer. *Stud Geophys Geod.* 1974;18(1):59–68.

Chen W, Huang Y, Wang Z, He R, Chen G, Li X. Horizontal and vertical motion at surface of a gassy ocean sediment layer induced by obliquely incident SV waves. *Eng Geol.* 2017;. doi:10.1016/j.enggeo.2017.01.001.

Chen WY, Xia TD, Sun MM, Zhai CJ. Transverse wave at a plane interface between isotropic elastic and unsaturated porous elastic solid half-spaces. *Transp Porous Med.* 2012;94(1):417–36.

Chen W, Wang Z, Zhao K, Chen G, Li X. Reflection of acoustic wave from the elastic seabed with an overlying gassy poroelastic layer. *Geophys J Int.* 2015;203(1):213–27. doi:10.1093/gji/ggv266.

Corredor RM, Santos JE, Gauzellino PM, Carcione JM. Reflection and transmission coefficients of a single layer in poroelastic media. *J Acoust Soc Am.* 2014;135(6):3151–62. doi:10.1121/1.4875713.

Dutta NC, Ode H. Seismic reflections from a gas-water contact. *Geophysics.* 1983;48(2):148–62. doi:10.1190/1.1441454.

Denneman AIM, Drijkoningen GG, Smeulders DMJ, Wapenaar K. Reflection and transmission of waves at a fluid/porous medium interface. *Geophysics.* 2002;67(1):282–91. doi:10.1190/1.1451800.

Feng SJ, Chen ZL, Chen HX. Reflection and transmission of plane waves at an interface of water/multilayered porous sediment overlying solid substrate. *Ocean Eng.* 2016;126:217–31. doi:10.1016/j.oceaneng.2016.09.009.

Garg SK, Nayfeh AH. Compressional wave propagation in liquid and/or gas saturated elastic porous media. *J Appl Phys.* 1986; 60(9):3045–55. doi:10.1063/1.337760.

Gurevich B, Schoenberg M. Interface conditions for Biot’s equations of poroelasticity. *J Acoust Soc Am.* 1999;105(5):2585–9. doi:10.1121/1.426874.

Kaynia AM, Banerjee PK. Fundamental solutions of Biot’s equations of dynamic poroelasticity. *Int J Eng Sci.* 1993;31(5):817–30. doi:10.1016/0020-7225(93)90126-F.

Kumar M, Saini R. Reflection and refraction of attenuated waves at the boundary of elastic solid and porous solid saturated with two immiscible viscous fluids. *Appl Math Mech Engl Ed.* 2012;33(6):797–816. doi:10.1007/s10483-012-1587-6.

Kumar M, Saini R. Reflection and refraction of waves at the boundary of non viscous porous solid saturated with single fluid and a

- porous solid saturated with immiscible fluids. *Lat Am J Solids Struct.* 2016;13(7):1299–324. doi:[10.1590/1679-78252090](https://doi.org/10.1590/1679-78252090).
- Kumar M, Sharma MD. Reflection and transmission of attenuated waves at the boundary between two dissimilar poroelastic solids saturated with two immiscible fluids. *Geophys Prospect.* 2013;61(5):1035–55. doi:[10.1111/1365-2478.12049](https://doi.org/10.1111/1365-2478.12049).
- Kumar M, Kumari M. Reflection of attenuated waves at the surface of a fractured porous solid saturated with two immiscible viscous fluids. *Lat Am J Solids Struct.* 2014;11(7):1206–37. doi:[10.1111/j.1365-246X.2010.04841.x](https://doi.org/10.1111/j.1365-246X.2010.04841.x).
- Kuo EYT. Acoustic wave scattering from two solid boundaries at the ocean bottom: reflection loss. *IEEE J Ocean Eng.* 1992;17(1):159–70.
- Lo WC, Sposito G, Majer E. Wave propagation through elastic porous media containing two immiscible fluids. *Water Resour Res.* 2005;41(2):1–25. doi:[10.1029/2004WR003162](https://doi.org/10.1029/2004WR003162).
- Lyu DD, Wang JT, Jin F, Zhang CH. Reflection and transmission of plane waves at a water–porous sediment interface with a double porosity substrate. *Transp Porous Med.* 2014;103(1):25–45.
- Paswan B, Sahu SA, Chattopadhyaya A. Reflection and transmission of plane wave through fluid layer of finite width sandwiched between two monoclinic elastic half-spaces. *Acta Mech.* 2016;227(12):3687–701. doi:[10.1007/s00707-016-1684-4](https://doi.org/10.1007/s00707-016-1684-4).
- Pride SR, Gangi AF, Morgan FD. Deriving the equations of motion for porous isotropic media. *J Acoust Soc Am.* 1992;92(6):3278–90. doi:[10.1121/1.404178](https://doi.org/10.1121/1.404178).
- Sahu SA, Paswan B, Chattopadhyay A. Reflection and transmission of plane waves through isotropic medium sandwiched between two highly anisotropic half-spaces. *Wave Random Complex.* 2015;26(1):42–67. doi:[10.1080/17455030.2015.1102361](https://doi.org/10.1080/17455030.2015.1102361).
- Santos JE, Ravazzoli CL, Carcione JM. A model for wave propagation in a composite solid matrix saturated by a single-phase fluid. *J Acoust Soc Am.* 2004;115(6):2749–60. doi:[10.1121/1.1710500](https://doi.org/10.1121/1.1710500).
- Sharma MD. Wave propagation across the boundary between two dissimilar poroelastic solids. *J Sound Vib.* 2008;314(3–5):657–71. doi:[10.1016/j.jsv.2008.01.023](https://doi.org/10.1016/j.jsv.2008.01.023).
- Sharma MD. Effect of local fluid flow on reflection of plane elastic waves at the boundary of a double-porosity medium. *Adv Water Resour.* 2013;61:62–73. doi:[10.1016/j.advwatres.2013.09.001](https://doi.org/10.1016/j.advwatres.2013.09.001).
- Sinha SB. Transmission of elastic waves through a homogeneous layer sandwiched in homogeneous media. *J Phys Earth.* 1964;12(1):1–4.
- Sharma MD, Kumar M. Reflection of attenuated waves at the surface of a porous solid saturated with two immiscible viscous fluids. *Geophys J Int.* 2011;184(1):371–84. doi:[10.1111/j.1365-246X.2010.04841.x](https://doi.org/10.1111/j.1365-246X.2010.04841.x).
- Tomar SK, Arora A. Reflection and transmission of elastic waves at an elastic/porous solid saturated by two immiscible fluids. *Int J Solids Struct.* 2006; 43: 7–8:1991–2013. Erratum 2007. *Int J Solids Struct.* 2006; 44:17:5796–5800. doi: [10.1016/j.ijsolstr.2007.05.021](https://doi.org/10.1016/j.ijsolstr.2007.05.021).
- Tuncay K, Corapcioglu MY. Wave propagation in poroelastic media saturated by two fluids. *J Appl Mech.* 1997;64(2):313–20. doi:[10.1115/1.2787309](https://doi.org/10.1115/1.2787309).
- Wang JT, Jin F, Zhang CH. Reflection and transmission of plane waves at an interface of water/porous sediment with underlying solid substrate. *Ocean Eng.* 2013;63:8–16. doi:[10.1016/j.oceaneng.2013.01.028](https://doi.org/10.1016/j.oceaneng.2013.01.028).
- Yeh CL, Lo WC, Jan CD, Yang CC. Reflection and refraction of obliquely incident elastic waves upon the interface between two porous elastic half-spaces saturated by different fluid mixtures. *J Hydrol.* 2010;395(1–2):91–102. doi:[10.1016/j.jhydrol.2010.10.018](https://doi.org/10.1016/j.jhydrol.2010.10.018).